3D Hemodynamics in Intracranial Aneurysms: Influence of Size and Morphology

Susanne Schnell[1], Sameer A Ansari[1,2], Parmede Vakil[1,3], Marie Wasilewski[1], Maria L. Carr[1], Michael C. Hurley[1,2], Bernard R. Bendok[2], Hunt Batjer[2], Timothy J. Carroll[1,3], James Carr[1], and Michael Markl[1,3]
[1]Radiology, Northwestern University, Chicago, Illinois, United States, [2]Neurological Surgery, Northwestern University, Chicago, Illinois, United States, [3]Biomedical Engineering, Northwestern University, Evanston, Illinois, United States

INTRODUCTION: Intracranial aneurysms (IAs) are diverse and life threatening conditions and occur in 3 to 6% of the population (1, 2). The annual rupture rate is approximately 2% (3) associated with significant morbidity and mortality. Current diagnostic methods for risk stratification and therapy planning are based on empirical parameters (e.g. patient age, aneurysm size, morphology, and location), ruptured or unruptured status, or systemic risk factors (hypertension, smoking/alcohol abuse etc.) (4,5) providing an incomplete assessment of a complex disease. Previous studies showed that also IA geometries, flow characteristics, and vessel wall properties can be substantially different for individual IAs (6). Also, IAs typically develop at major bifurcation sites suggesting that complex blood flow patterns may have a major influence on pathogenesis. To date, no systematic evaluation of the impact of IA morphology, size and location on in-vivo aneurysmal 3D flow characteristics has been performed. This study provides a comprehensive in-vivo quantification of hemodynamic parameters including intra-IA 3D velocity distribution, vorticity, and wall shear stress (WSS) in a cohort of 18 IA patients using cardiac-gated 4D flow MRI.

METHODS: Cerebral 4D flow MRI (spatial resolution=0.99–1.8x0.78–1.46x1.2–1.4mm^3, temporal resolution=44–48ms, total scan time=15–20min) was performed on 1.5T and 3T systems (Avanto & Trio, Siemens, Germany) in 18 patients (age=55.4±13.8 years) with 19 IAs. Aneurysms had saccular (n=16) and fusiform (n=3) morphology and different sizes ranging from small (n=8, largest dimension=6.2±0.4mm) to large and giant (n=11, 25±7mm). The patients represented three different groups of aneurysms based on IA size and morphology as summarized in Figure 1. Data analysis further included visualization of intra-aneurysmal flow patterns (3D pathlines, color-coded 2D vector graphs) as well as 3D segmentation of the aneurysm and quantification of spatial-temporal 3D velocity distribution, vorticity, and WSS along the aneurysms 3D surface. To assess the 3D velocity distribution, the velocities were arranged in a histogram and normalized by the total number of voxels in the segmented volume. The relative absolute vorticity was defined as $Vort = \mathrm{abs}(\zeta x, \zeta y, \zeta z)$ (with $\zeta x = \delta w/\delta y - \delta v/\delta z$, $\zeta y = \delta u/\delta z - \delta w/\delta x$, $\zeta z = \delta v/\delta x - \delta u/\delta y$ and u,v,w being the vector components of the velocity) and was calculated within a 2D plane transecting the aneurysm. WSS was calculated by cubic spline interpolation of the velocity gradient along the aneurysm contour as described previously (8, 9).

RESULTS: As shown in Figures 1 and 2, flow visualization and quantification (vorticity, 3D velocity distribution, and WSS along the aneurysms surface wall) revealed distinct hemodynamic patterns for large/giant saccular aneurysms (Group 1), small saccular aneurysms (Group 2) and large/giant fusiform aneurysms (Group 3). Group 1 IAs demonstrated a narrow high-flow channel along the aneurysm wall in combination with large central slow flow regions. Aneurysms in Group 2 showed more prominent high-flow channels peripherally with smaller central slow flow regions. In contrast, slow flow with less defined flow channels were noted in the fusiform IAs (Group 3).

Consistent with these observations, Groups 1 and 2 had the significantly higher peak velocities ($p<0.002$) and an increased mean WSS ($p<0.001$) (figure 2). Although velocity distributions and mean velocities were similar for Group 1 and 2, vorticity and WSS was significantly ($p<0.001$) increased in Group 1 compared to Group 2 (both by about 54%) indicating a relationship between IA size, hemodynamics and wall forces. Group 3 showed generally reduced mean and peak velocities ($p<0.001$) and the lowest WSS ($p<0.001$).

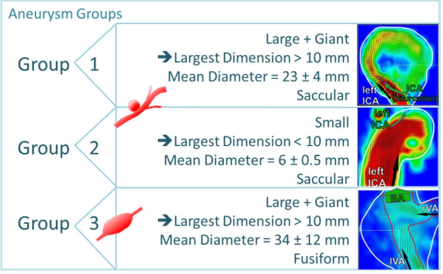

Figure 1: Left: Schematic group description and demographics. **Right:** Representative intra-aneurysmal flow visualization in IAs for all Groups. Note the inter-group differences in high in-flow channels and low flow regions resulted in significant differences in 3D velocity distribution and WSS (Figure 2).

DISCUSSION AND OUTLOOK: Characterization of IA aneurysm 3D blood flow demonstrated the influence of lesion size and morphology on hemodynamics suggesting the potential of 4D flow MRI to assist in the classification of individual aneurysms. Due to its ability to detect subtle hemodynamic changes and the possibility to differentiate aneurysm types, 4D flow MRI may have the potential to aid risk stratification by associating differences in WSS and intra-aneurysmal 3D velocity distribution with risk of rupture. Future longitudinal studies and correlation with patient outcome are needed to evaluate the utility of the identified quantitative markers of intra-aneurysmal hemodynamics for improved risk assessment and therapy planning.

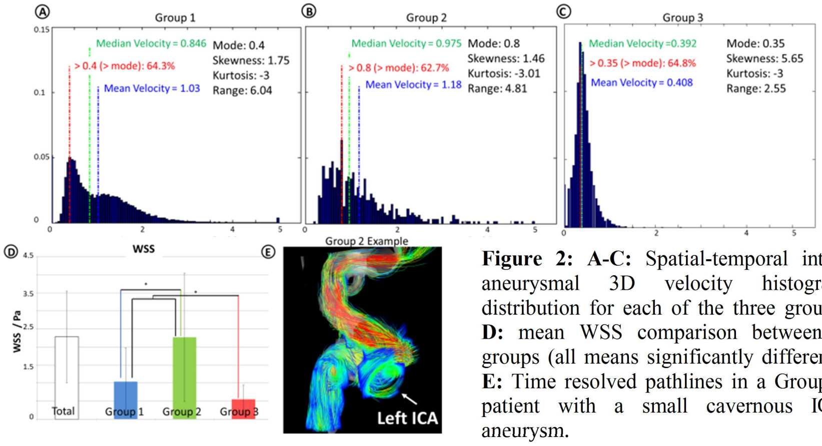

Figure 2: A-C: Spatial-temporal intra-aneurysmal 3D velocity histogram distribution for each of the three groups. **D:** mean WSS comparison between 3 groups (all means significantly different). **E:** Time resolved pathlines in a Group 2 patient with a small cavernous ICA aneurysm.

REFERENCES: (1) Chen et al. Neurosurgical Focus, 2004, (2) King et al. Neuroimaging clinics of Northamerica 1997, (3) Rinkel et al. Stroke 1998, (4) Rahman et al. Stroke 2010, (5) Wardlaw and White Brain 2000, (6) Sforza et al. Annual review of fluid mechanics 2009, (7) Stalder et al. MRM 2008, (8) Meckel et al. Neuroradiology 2008

ACKNOWLEDGEMENTS: The work was supported by the German Research Foundation SCHN 1170/2-1, SIR Foundation Pilot Research Grant, RSNA Research Seed Grant, grant RSD1207, NIH T32 EB005170 and NIH R01 HL088437.